Available online at www.sciencedirect.com

SCIENCE DIRECT®

Physics Letters A 320 (2004) 322–326

PHYSICS LETTERS A

www.elsevier.com/locate/pla

Determination of the polarity of ZnO thin films by electron energy-loss spectroscopy

Y. Wang [a,*], Q.Y. Xu [a], X.L. Du [b], Z.X. Mei [b], Z.Q. Zeng [b], Q.K. Xue [b], Z. Zhang [a,c]

[a] *Beijing Laboratory of Electron Microscopy, Institute of Physics and Center for Condensed Matter Physics, Chinese Academy of Sciences, P.O. Box 603, Beijing 100080, China*

[b] *State Key Laboratory for Surface Physics, Institute of Physics, Chinese Academy of Sciences, Beijing 100080, China*

[c] *Beijing University of Technology, 100 Pingle Yuan, Chao Yang District, Beijing 100022, China*

Received 24 August 2003; accepted 14 November 2003

Communicated by J. Flouquet

Abstract

The polarity of the ZnO film grown on sapphire using an ultra-thin Ga wetting layer has been investigated by electron energy-loss spectroscopy (EELS). The intensity of the oxygen K-edge in electron energy-loss spectrum from the ZnO film shows a prominent difference when the film orientation changes from the (0002) Bragg condition to the (000$\bar{2}$) Bragg condition. The EELS study reveals that the ZnO film with very thin Ga wetting layer has the [0001] polarity, which is further confirmed by the conventional convergent beam electron diffraction method.
© 2003 Elsevier B.V. All rights reserved.

PACS: 79.20.Uv; 61.14.Lj; 73.61.Ga; 68.55.Jk

Keywords: Polarity; EELS; Zinc oxide; Oxygen K-edge

In the last few years wurtzite ZnO and related alloys have attracted great attention because of their potential applications in light-emitting diodes and diode lasers operating in the short wavelength of the visible spectrum [1]. In these non-centrosymmetric materials, polarity that results from the stacking sequence of the (0001) atomic planes in wurtzite-type ZnO and MgZnO, or the (111) planes in rock-salt-type MgO and ZnMgO, has strong influences on growth process, surface morphology and electronic properties [2,3]. Several TEM methods such as energy-dispersive X-ray spectroscopy [4], convergent beam electron diffraction (CBED) [5,6], high-resolution TEM [7] and electron energy-loss spectroscopy (EELS) [2,8], have been developed for polarity determination. Among these methods, CBED is the popular method used to determine the polarity. However, as the CBED pattern is sensitive to the defects in the illuminated area of the specimen, the use of this method is sometimes limited [2]. EELS provides a more sensitive way to investigate the polarity of a non-centrosymmetric crystal [2]. The inelastically scattered electrons with an energy loss of E are concentrated within a cone of semiangle $\theta_E = E/2E_0$, the characteristic angle for

* Corresponding author.
E-mail address: ywang@blem.ac.cn (Y. Wang).

0375-9601/$ – see front matter © 2003 Elsevier B.V. All rights reserved.
doi:10.1016/j.physleta.2003.11.032

inelastic scattering, the value for oxygen K-edge is about 1.3 mrad as $E_0 = 200$ keV. A large fraction of the electrons that contain information about an inner-shell ionization can be collected and analyzed with a proper collection angle [9,10]. In this Letter, we apply this technique to determine the polarity of the ZnO film prepared using an ultra-thin Ga wetting layer as a transition layer between the sapphire (0001) substrate and epitaxial ZnO film.

The sample for this study was grown by radio frequency plasma-assisted molecular beam epitaxy (MBE-IV, ShengYang KeYI) on sapphire (0001) substrate. Zinc (gallium) atomic beam was supplied by evaporating 6N (7N) elemental Zn (Ga) from a commercial Knudsen cell. Active oxygen radicals were produced by an RF-plasma system (HD25R, Oxford Applied Research). After the substrate was pretreated in the growth chamber using oxygen plasma exposure for 30 min, an ultra-thin Ga wetting layer was deposited on the oxygen-terminated sapphire (0001) surface under ultra-high vacuum condition with a gas pressure about 3×10^{-7} Pa. The Ga layer was used to modify the sapphire surface. Consequently, the ZnO film was grown on the Ga-terminated surface, rather than the usual Al- or O-terminated one. The monolayer number of the Ga layer was controlled precisely by the Ga exposure time and Ga-cell temperature. The role of the Ga wetting layer in the defect reduction and rotation domain elimination in ZnO epilayer has been discussed by Du et al. [11] and Wang et al. [12]. The cross-sectional transmission electron microscopy (XTEM) specimen for EELS observation was prepared by the conventional method including cutting, gluing, mechanical polishing, dimpling procedures and then followed by the Ar^+ ion-beam milling to perforation. A Philips CM200 field emission gun TEM equipped with a Gatan image filtering (GIF) system was operated at 200 kV to carry out the EELS experiment. The energy resolution is about 1.0 eV according to the measured full width at half maximum of the zero-loss peak. In our experiments, a zero-loss spectrum and the corresponding core-shell ionization edge EELS spectrum was obtained consecutively from the same region and dealt with using EL/P 3.0 software. The cross-sectional sample was tilted to the Bragg position of either (0002) or $(000\bar{2})$, and away from any zone axis but satisfying two-beam condition. The EELS spectra were acquired with an off-axis collection aperture of about 3 mrad collection semi-angle. The thickness of the area chosen for observation was estimated to be 100 nm, as obtained from low-loss spectrum analysis [9]. The EELS spectra are with background subtracted according to the power law, and the multiple-inelastic-scattering effect removed using the Fourier ratio (for deconvolution) technique. The Zn $L_{2,3}$-edge spectra are normalized to compare the two O K-edge intensities. It is obvious that the O K-peak has a relatively higher intensity at the (0002) Bragg orientation than that at $(000\bar{2})$, as shown in Fig. 1. The difference between the two O K-edge peaks is not very prominent. It is because the sample thickness of the field we studied is about $1.35\xi_{0002}$ ($\xi_{0002} \approx 75$ nm) [10]. It deviates from the optimum sample thickness $0.4\xi_{0002}$ at which the difference is estimated to be maximum [2].

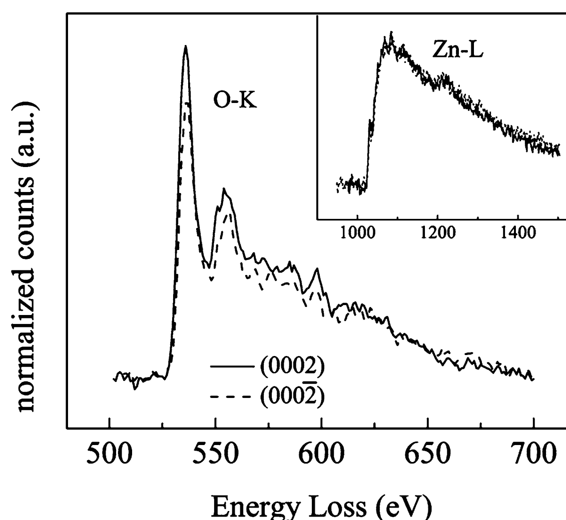

Fig. 1. Comparison of the normalized O K-edges acquired at (0002) and $(000\bar{2})$ Bragg conditions. The inset is the normalized Zn L-edges.

Now we apply the two-beam theory for acentric crystals to clarify the EELS result and determine the polarity of the ZnO film. At the two-beam condition, the thickness-averaged electron current density (TAECD) at exact Bragg condition g, without absorption, has been given as [2,4]:

$$I(r) = 1 - \frac{1 - \cos(2\pi t')}{2\pi t'} \sin\left[2\pi(gr + \varphi)\right],$$

where the thickness is given in terms of the two-beam extinction distance, i.e., $t' = t/\xi g$ (t denotes

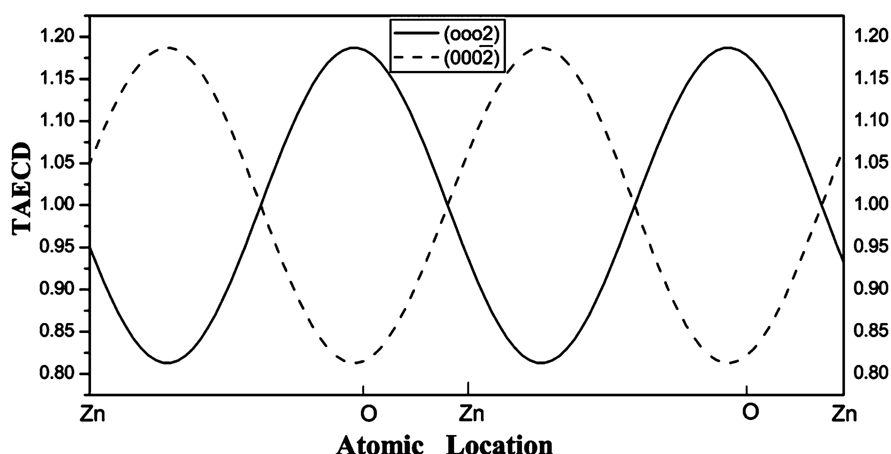

Fig. 2. The calculated thickness-averaged electron current densities across a unit cell at (0002) and (000$\bar{2}$) Bragg conditions, respectively. The sample thickness is $1.35\xi_{0002}$.

the thickness of the sample and ξg denotes the two-beam extinction distance). Here r is the coordinate of the atomic planes ($r = 0$ for the Zn plane, and $r = 0.3844$ for the O plane), and φ is the phase shift due to the absence of a center of symmetry. Fig. 2 shows, the profiles of the thickness-averaged electron current density (TAECD) versus the atomic planes position at (0002) and (000$\bar{2}$) Bragg conditions, for a sample thickness of $1.35\xi_{0002}$. Here we assume the Zn atomic plane location is zero, whereas the O atomic plane position is 0.3844 nm (calculated according to Jeffrey's suggestion [13]), which is around the peak or valley position in term of the Bragg condition. It is clear that near the O planes the difference is the largest, but around the Zn planes it becomes to be zero. This indicates that the O K-edge taken at the (0002) Bragg condition should be higher than that at the (000$\bar{2}$) Bragg condition when the spectra are normalized using the Zn L-edges. The experimental result shown in Fig. 1 is in good agreement with the theoretical calculation. Although the magnitude of the difference of the O K-edge is relatively small due to the influence of the sample thickness, it will not change the relatively intensity of the O K-edges of the two Bragg conditions and thus the result of the film polarity determination [2]. Using this criterion, we can clearly index both (0002) and (000$\bar{2}$) diffraction disks in the CBED pattern of the ZnO film. It is well known that the shadow images will be unrotated in an over-focused CBED pattern and 180°-rotated in an under-focused CBED pattern [14,15]. In the case of over-focused CBED, the sample is situated below the object plane (where the beam is focused), and thus, the simple ray path of electrons indicates there will be no 180° rotation between the shadow images and the electron diffraction disks [14,15]. Fig. 3(a) shows an over-focused CBED pattern near the [11$\bar{2}$0] zone axis and the shadow image of the ZnO film in the diffraction disks is clearly seen, where the rugged side denotes the surface of ZnO film. The diffraction disks have been indexed using the above-mentioned EELS method, and then, the ZnO film with very thin Ga wetting layer is determined to have the [0001] polarity.

To confirm our EELS result, we also carry out a CBED experiment. The CBED pattern was taken by a FEG-CM200 operating at 200 kV, with a 50 μm C2 condensed aperture and a 960 mm camera length. In order to find the dislocation-free regions in sample for the CBED experiments, the defect structures were studied with cross-sectional TEM images, which were taken by a Philips CM12 TEM at 100 kV. Few straight plane defects (e.g., inversion domains) are observed. The main defects are threading dislocations, as reported by the other group [16]. The details of the defect characterization of this sample will be discussed elsewhere [12]. As seen in Fig. 3(b), some dislocation-free regions were selected to carry out the CBED experiment. The CBED pattern was taken near to [1$\bar{1}$00] zone axis, with a small angle away from the axis toward [1$\bar{2}$10] direction. In this case, the electron diffraction from $(0002)_{Zn}$ and $(000\bar{2})_{O}$ faces could be still distinguished by the fringes in the

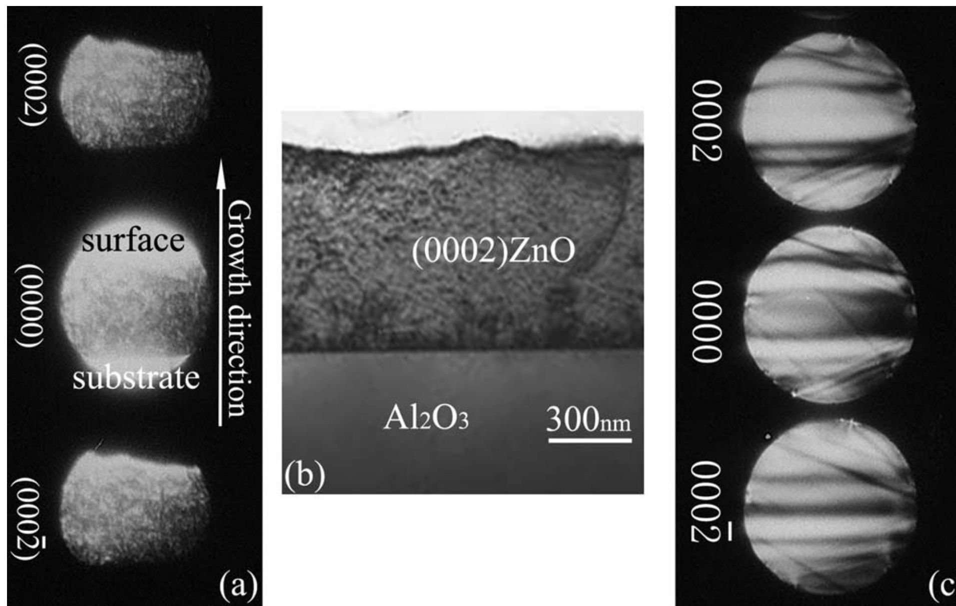

Fig. 3. The shadow images of the ZnO film near [11$\bar{2}$0] zone in the over focused CBED pattern (a) and a bright field XTEM image of the ZnO film with $g = 0002$ (b) with the corresponding CBED pattern (c).

CBED disk, as shown in Fig. 3(c), which are similar to the pattern of GaN [6]. Since the $(0002)_{Zn}$ face can reflect the electron beam much more strongly than the $(000\bar{2})_{O}$ face, the centre fringes at (0002) and (000$\bar{2}$) disks should be bright and dark, respectively. And the fringes in (0000) disk are symmetrical because the electron beam was exactly parallel to the (0001) plane [6]. Thus, we can ensure the tokens in the CBED pattern of the ZnO film and the ZnO film have a [0001] polarity.

The substrate pretreatment and the initial growth procedure have a strong influence on polarity selection of subsequent ZnO film because the polarity of ZnO film is determined by the stacking sequence of the atomic planes at the initial growth stage. An oxygen-terminated sapphire (0001) surface can be formed by plasma-excited oxygen pretreatment. At the very beginning of ZnO growth, Zn atoms in the first ZnO layer will form strong bonds with the underlying O atoms on the topmost sapphire surface. As a result, the [000$\bar{1}$] polarized ZnO film should be observed, as reported previously [16,17]. Since the oxygen-terminated sapphire (0001) surface is not stable in vacuum condition [18], small part of the surface is Al-terminated, which leads to formation of inversion domains in the ZnO film [19]. In order to suppress inversion domains formation, the sapphire (0001) surface is modified with a few monolayers of Ga. On this Ga-terminated surface, a deposition sequence of Ga–O–Zn should be energetically favorable, and a solely Zn-polarized ZnO film will be resulted, as demonstrated in our EELS and CBED study. High-resolution TEM observation also shows that the inversion domains and defect density in the ZnO film are reduced greatly, which significantly improves the crystal quality, electrical and optical properties of the film [11,12]. It has been reported that polarity inversion in GaN films can be achieved using surface modification by a few monolayers of Mg [20] or Al [21], which is analogical to the result reported in this Letter. In our case, the thin Ga wetting layer changes the interface bonding configuration and inverts the atomic sequencing from the Zn–O–Zn– to the O–Zn–O–. Since the quality of the ZnO film with [0001] polarity is better [3], surface modification using a thin metallic layer such as Ga is recommended to control the polarity of the ZnO epilayer and improve its properties.

In summary, the [0001] polarity of the ZnO film grown on sapphire (0001) surface with an ultra-thin Ga wetting layer has been determined by EELS. The difference between the thickness-average electron current intensities at the (0002) and (000$\bar{2}$) Bragg

conditions leads to a prominent difference of the intensity of the O K-edge in the electron energy-loss spectra. Thus the indexing of the (0002) and $(000\bar{2})$ reflections can be carried out by comparison of the intensity of the O K-edge, and then, the polarity of the ZnO film can be determined by combining the shadow image in the over focused CBED pattern. The [0001] polarity of the ZnO film is confirmed independently by conventional CBED method.

Acknowledgements

This work was supported by National Natural Sciences Foundation of China (Grant Nos. 60271028, 60021403 and 60376004) and by Ministry of Science and Technology of China (2002CB613500).

References

[1] T. Mitate, Y. Sonoda, N. Kuwano, Phys. Status Solidi A 192 (2002) 383.
[2] X. Kong, G.Q. Hu, X.F. Duan, Y. Lu, X.L. Liu, Appl. Phys. Lett. 81 (2002) 1990.
[3] S. Hong, T. Hanada, H. Ko, Y. Chen, T. Yao, D. Imai, K. Araki, M. Shinohara, K. Saitoh, M. Terauchi, Phys. Rev. B 65 (2002) 115331.
[4] N. Jiang, T.J. Eustis, J. Cai, F. Ponce, J.C.H. Spence, J. Silcox, Appl. Phys. Lett. 80 (2002) 389.
[5] B. Daudin, J.L. Rouvière, M. Arlery, Appl. Phys. Lett. 69 (1996) 2480.
[6] P. Han, Z. Wang, X.F. Duan, Z. Zhang, Appl. Phys. Lett. 78 (2001) 3974.
[7] P. Vermaut, P. Ruterana, G. Nouet, Philos. Mag. A 76 (1997) 1215.
[8] J. Taftø, Acta Crystallogr. A 43 (1987) 208.
[9] R.F. Egerton, Electron Energy Loss Spectroscopy in the Electron Microscope, 2nd Edition, Plenum Press, New York, 1996.
[10] D.B. Williams, C.B. Carter, Transmission Electron Microscopy: A Textbook for Materials Science, Plenum Press, New York, 1996.
[11] X.L. Du, M. Murakami, H. Iwaki, Y. Ishitani, A. Yoshikawa, Jpn. J. Appl. Phys. 41 (2002) L1043.
[12] Y. Wang, Q.Y. Xu, Y.G. Wang, X.L. Du, Q.K. Xue, Z. Zhang, unpublished.
[13] T.M. Sabine, S. Hogg, Acta Crystallogr. B 25 (1969) 2254.
[14] J.P. Morniroli, F. Gaillot, Ultramicroscopy 83 (2000) 227.
[15] Ch. Jäger, E. Spiecker, J.P. Morniroli, W. Jäger, Ultramicroscopy 92 (2002) 273.
[16] F. Vigué, P. Vennéguès, S. Vézian, M. Laügt, J.-P. Faurie, Appl. Phys. Lett. 79 (2001) 194.
[17] T. Ohnishi, A. Ohtomo, M. Kawasaki, K. Takahashi, M. Yoshimoto, Appl. Phys. Lett. 72 (1998) 824.
[18] C. Noguera, J. Phys.: Condens. Matter 12 (2000) R367.
[19] P. Fons, K. Iwata, A. Yamada, K. Matsubara, S. Niki, Appl. Phys. Lett. 77 (2000) 1801.
[20] V. Ramachandran, R.M. Feenstra, W.L. Sarney, L. Salamanca-Riba, J.E. Northrup, L.T. Romano, D.W. Greve, Appl. Phys. Lett. 75 (1999) 808.
[21] D.H. Lim, K. Xu, S. Arima, A. Yoshikawa, K. Takahashi, J. Appl. Phys. 91 (2002) 6461.